

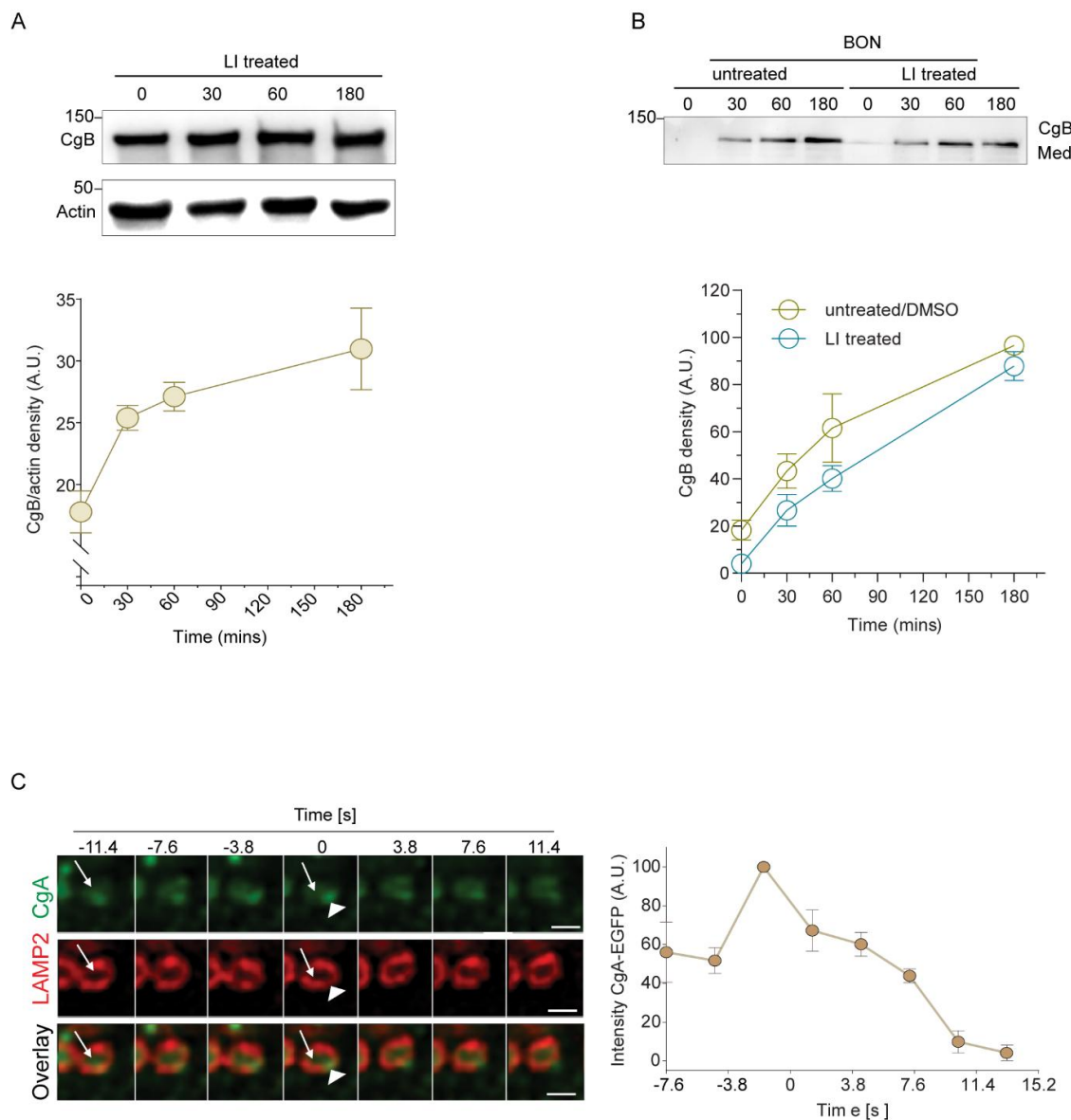
**Molecular requirements for mammalian crinophagy highlight a key role for  $\text{Ca}^{2+}$ -dependent Munc13-4**

Muralidharan Mani<sup>1</sup>, Declan J. James<sup>1,2</sup> and Thomas F.J. Martin<sup>1</sup>

<sup>1</sup>Department of Biochemistry, University of Wisconsin-Madison, Madison, WI, USA, 53706. Tel. + 1 6082632427. *Correspondence:* [mmani3@wisc.edu](mailto:mmani3@wisc.edu), [tfmartin@wisc.edu](mailto:tfmartin@wisc.edu)

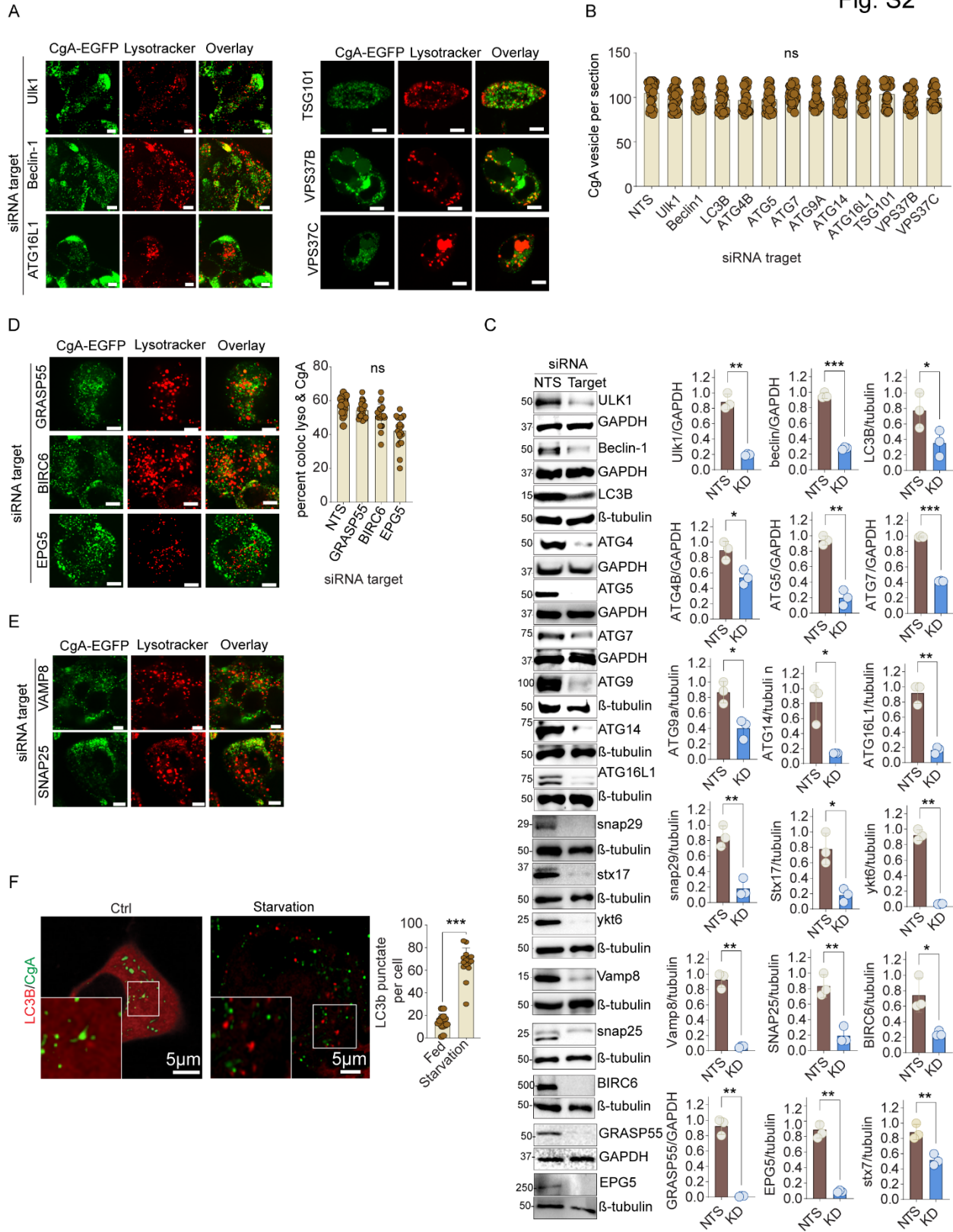
<sup>2</sup>Current address: Gene and Cell Therapy, GMP, PPD Clinical Research Business of Thermo Fisher Scientific, 8551 Research Way, Suite 90, Middleton, WI, USA, 53562. [Declan.James@ppd.com](mailto:Declan.James@ppd.com).

Fig. S1



**Fig S1. SG turnover in neuroendocrine cells.** A. BON cells were treated with LIs (pepstatin 1  $\mu$ M and 1  $\mu$ M E64D) for 0, 30, 60, and 180 min and western blot analysis of CgB in total cell lysate was conducted. The plotted data represent mean  $\pm$  SD. B. BON cells were treated with DMSO or LIs for 0, 30, 60, and 180 min and western blot analysis was conducted for CgB secreted in media from three independent experiments. The plotted data represent mean  $\pm$  SD. C. CgA-EGFP stable BON cells were transiently transfected with LAMP2-mCherry and were imaged using confocal microscopy. Frames were captured every 3.8 seconds. The intensity of the CgA-EGFP in the lysosomal lumen was plotted (n=5). Arrowhead indicates CgA contact with the lysosome (at time zero), and the arrow indicates the lysosomal lumen. Scale Bar, 5  $\mu$ m.

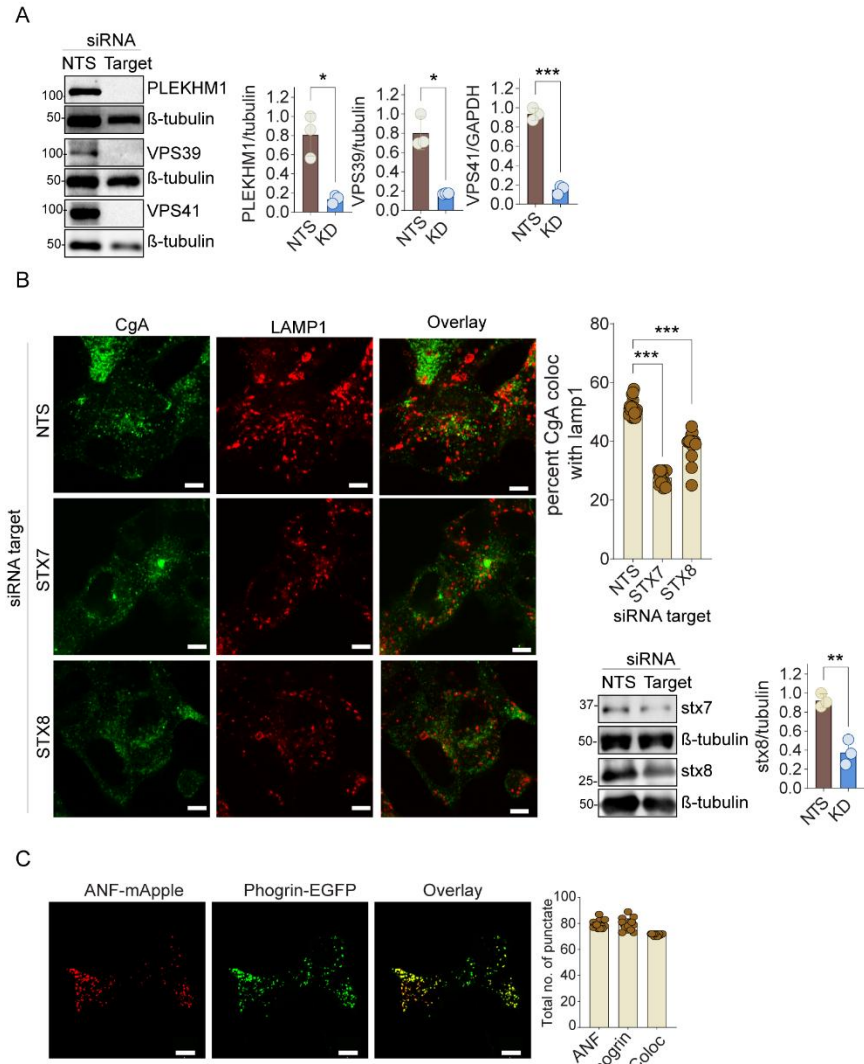
Fig. S2



**Fig S2. Macroautophagy is dispensable for SG degradation. A. Additional macroautophagy**

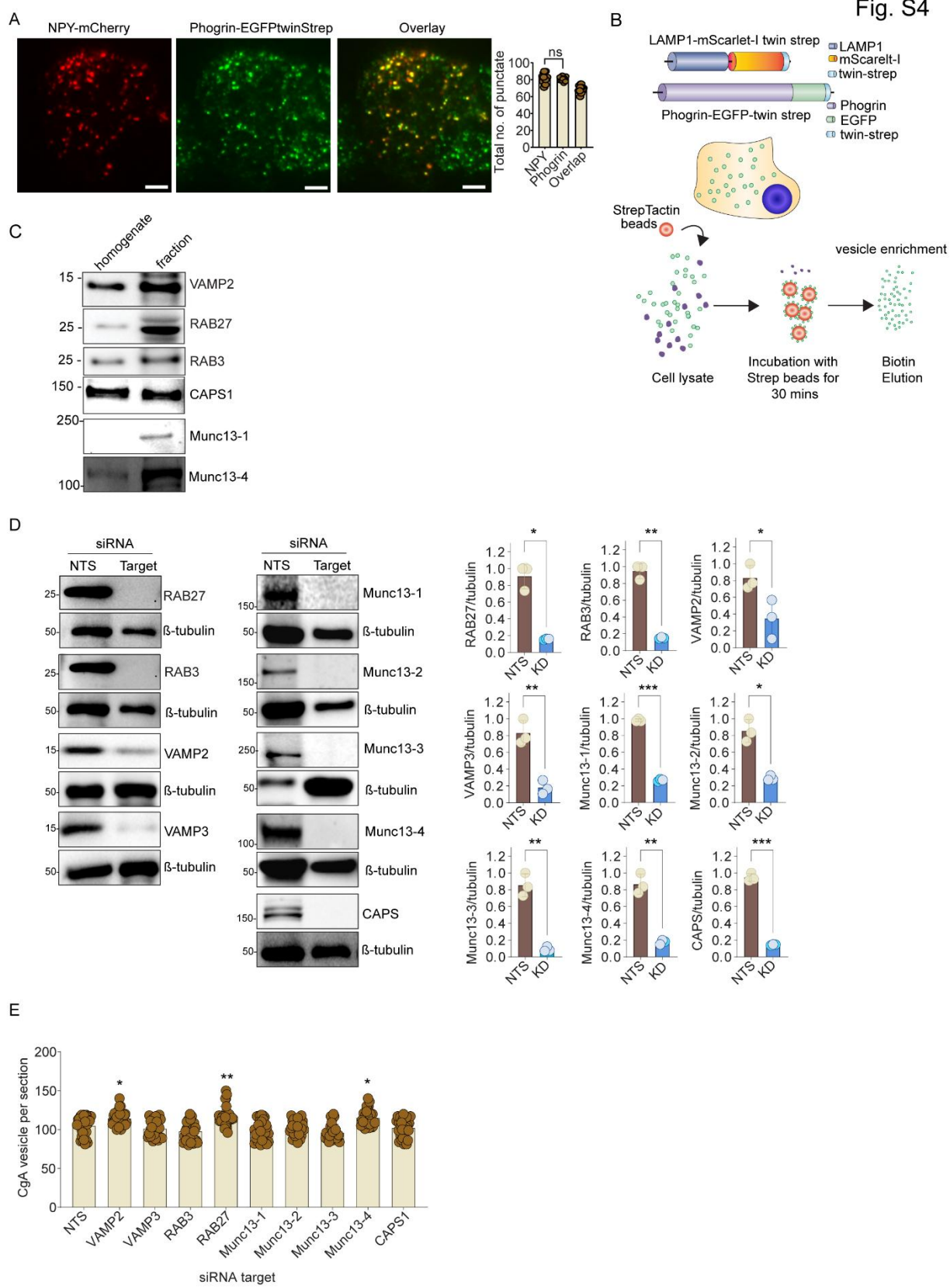
proteins Ulk1, Beclin1, ATG16L1, and the microautophagy proteins Tsg101, VPS37B, VPS37C are dispensable for SG-lysosome merge in resting BON cells. Data and analysis in Fig 2C. B. Quantitation of CgA SGs per confocal section in ATG-depleted samples (n = 35, N = 3, ns). C. Western blot analysis of selective gene knockdown of Ulk1, Beclin1, LC3B, ATG 4B, ATG5, ATG7, ATG9A, ATG14 and ATG16L1, SNAP29, STX17, YKT6, VAMP8, SNAP25, BIRC6, GRASP55, EPG5, STX7, STX8 (n = 35, N = 3, mean  $\pm$  SD \*p<0.1, \*\*p< 0.01, \*\*\*p<0.001). D. The major tethers involved in macroautophagy (GRASP55, BIRC6, and EPG5) are dispensable for SG degradation in resting BON cells. Quantitation of lysotracker red with CgA-GFP colocalization after gene knockdown (n = 35, N = 3, mean  $\pm$  SD, ns) (Scale Bar, 5  $\mu$ m). E. siRNAs were used to deplete VAMP8 or SNAP25 in CgA-EGFP stable BON cells that were labeled with lysotracker red (see Fig 2C). F. CgA-EGFP stable BON cells transfected with LC3-mApple were imaged after 4 hrs of normal medium or starvation (n= > 15, mean  $\pm$  SD, \*\*\*p <0.001) (Scale Bar, 5  $\mu$ m).

Fig. S3



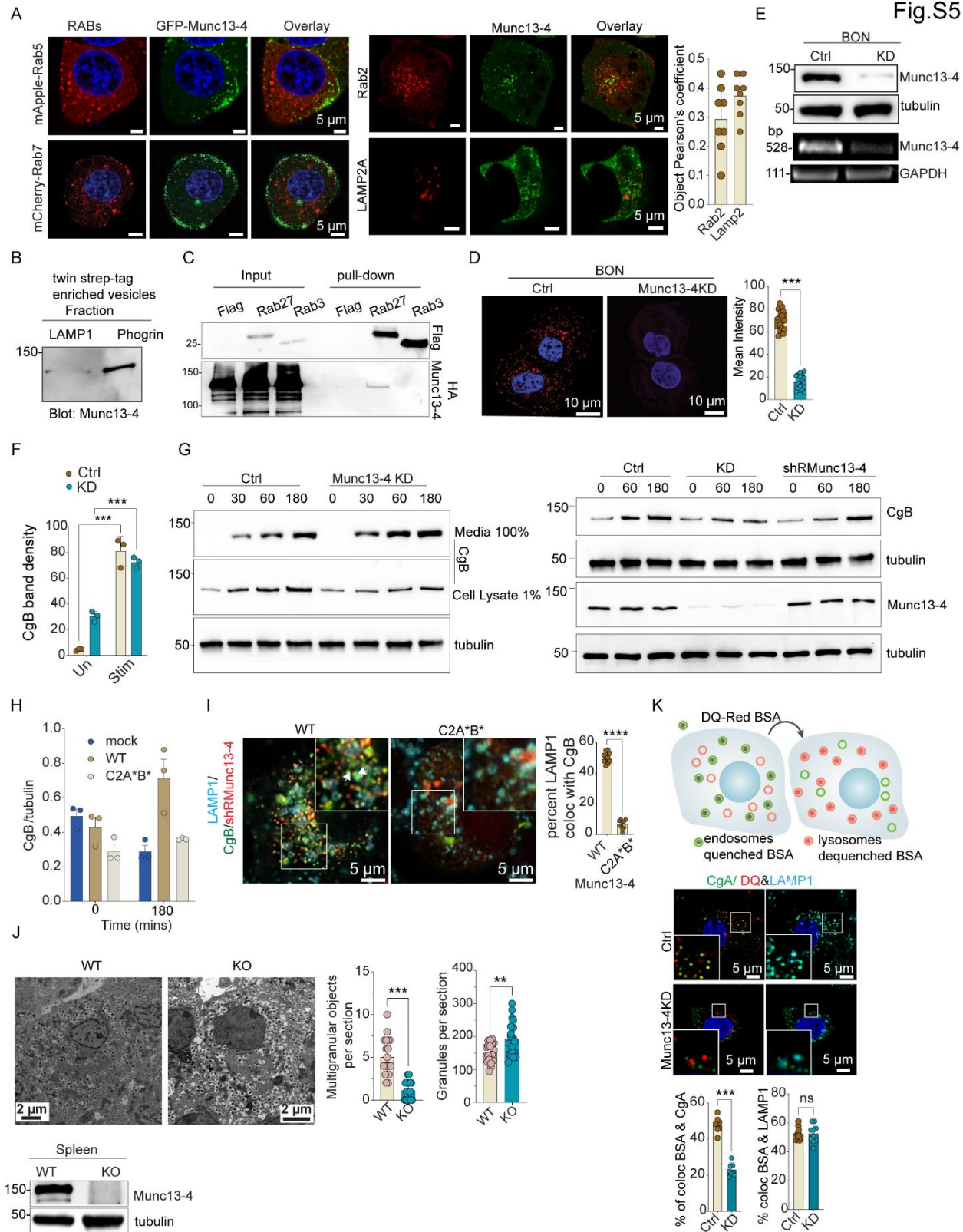
**Fig S3. Lysosomal tethering proteins and SNAREs involved in SG-lysosome fusion. A.** Western blot analysis of selective gene knockdown of PLEKHM1, VPS39, and VPS41 (N=3, mean  $\pm$  SD, \* p <0.1, \*\*\* p <0.001. **B.** BON cells were treated with indicated siRNAs for 72 h and cells were immunostained with CgA and LAMP1 after LI treatment for 4 hours. Endogenous LAMP1 and CgA colocalization was quantitated after selective gene knockdown. Quantitation of LAMP1 (red) with CgA-GFP (green) colocalization after gene knockdown (n = 15, N = 3, mean  $\pm$  SD, ns) (Scale Bar, 5  $\mu$ m). A significant reduction in LAMP1-CgA colocalization was observed in STX7- and STX8-depleted samples compared to NTS samples. Western blot analysis and quantification of STX7 and STX8 siRNA knockdown (N = 3, mean  $\pm$  SD, \*\* p <0.01). **C.** Phogrin-EGFP was well colocalized with the SG marker ANF-mApple. The total number of ANF-mApple, Phogrin-EGFP, and colocalized puncta per cell were quantitated (n = 15, mean  $\pm$  SD) (Scale Bar, 5  $\mu$ m).

Fig. S4



**Fig S4. SG resident proteins and SNAREs involved in SG-lysosome fusion.** A. Co-expression of NPY-mCherry and Phogrin-EGFP twin strep tag in BON cells. The total number of Phogrin-EGFP, ANF-mApple, and overlap clusters was manually determined ( $n = 15$ , mean  $\pm$  SD) (Scale Bar, 5  $\mu$ m). B. Single-step enrichment of SGs was conducted by expressing Phogrin-EGFP-twin strep and processing lysates on StrepTactin beads as indicated. C. Western blot analysis of ~2 percent of homogenate and ~4 percent equivalent enriched SG fraction. D. Western blot analysis for siRNA knockdown of RAB27A, RAB3A, VAMP2, VAMP3, Munc13-1, Munc13-2, Munc13-3, Munc13-4, and CAPS1 ( $N = 3$ , mean  $\pm$  SD, \*  $p < 0.1$ , \*\*  $p < 0.01$ , \*\*\*  $p < 0.001$ ). E. Quantitation of CgA SGs per confocal section for the indicated siRNA-targeted BON cell samples ( $n = 35$ ,  $N = 3$ , mean  $\pm$  SD, \*  $p < 0.1$ , \*\*  $p < 0.01$ , ns).

Fig.S5

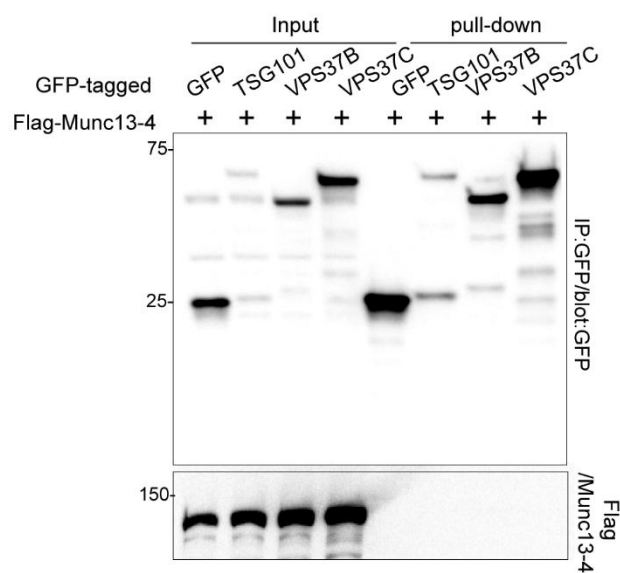


**Fig S5. Distribution of Munc13-4 on SGs and its depletion affects in SG turnover. A.** Expression of EGFP-Munc13-4 with organelle markers for endosomes (mApple-Rab5), late

endosomes (mCherry-Rab7), ERGIC (mCherry-Rab2) and lysosomes (LAMP2-mCherry) exhibited little colocalization as indicated (quantitation see Fig 5A) (n = 15) (Scale bar, 5  $\mu$ m). B. Western blot analysis was conducted on Phogrin-enriched and LAMP1-enriched BON cell fractions. Munc13-4 was detected in the Phogrin-enriched fraction. C. Lysates prepared from BON cells expressing Flag, Flag-Rab27A, or Flag-Rab3A co-expressed with HA-Munc13-4 were immunoprecipitated with a FLAG antibody followed by immunoblotting with HA and Flag antibody. D. Immunostaining of Munc13-4 in Ctrl and Munc13-4 KD BON cells and the mean intensity signals Munc13-4 in Ctrl and KD cells (n = 15,  $\pm$  SD, \*\*\* p < 0.001) (Scale Bar, 10  $\mu$ m). E. Western blot analysis of Munc13-4 and tubulin in Ctrl and Munc13-4 KD cells. PCR amplified Munc13-4 and GAPDH RNAs were separated by agarose gel electrophoresis. F. Slot blot analysis was conducted to quantitate CgB collected in media from Ctrl or KD cells following incubations in basal conditions (Un) or with 1.25  $\mu$ M ionomycin (Stim) (n = 3, mean  $\pm$  SD, \*\*\* p < 0.001). G. BON cells (Ctrl or Munc13-4 KD or shRNA resistant Munc13-4) were treated with LIs for the indicated time. Cell lysate and complete media were subjected to western blot analysis using CgB and tubulin antibodies (quantitation see Fig 5C). H. Munc13-4 KD BON cells were transfected with mock, wild-type, or C2A\*B\* Munc13-4 plasmids, treated with LIs, and analyzed by western blot for CgB and tubulin. CgB/tubulin ratios were quantitated from triplicate experiments (n = 3, mean  $\pm$  SD, \*\*\*p < 0.001, ns). I. BON Munc13-4-depleted cells were transfected with shRNA-resistant mCherry Munc13-4 WT or C2A\*B\* plasmids mutants. Cells were treated with LIs for 4h and fixed for immunostaining with CgB and LAMP1 antibodies (n = 15, mean  $\pm$  SD, \*\*\*\* p < 0.0001) (Scale Bar, 5  $\mu$ m). J. Pancreatic  $\beta$ -cells from wildtype mice and mice lacking Munc13-4 protein were cultured in RPMI with 5.5 mM glucose for seven days. Electron microscope analysis of pancreatic  $\beta$ -cells treated with LIs for 4-6 hrs. The number of multigranular bodies and insulin granules per section was counted across 35 images (n = 3 per group, mean  $\pm$  SD, \*\* p < 0.01, \*\*\* p < 0.001). Munc13-4 and tubulin protein levels from the spleen were examined by western blot for Munc13-4 wildtype and KO. K. Confocal microscopy of BON cells (Ctrl or KD) that were incubated with DQ-BSA for 30 min and immunostained with CgB and LAMP1 antibodies. The overlap of dequenched DQ-BSA with CgA or LAMP1 was quantitated (n = 15 per group, mean  $\pm$  SD, ns, \*\*\* p < 0.001).

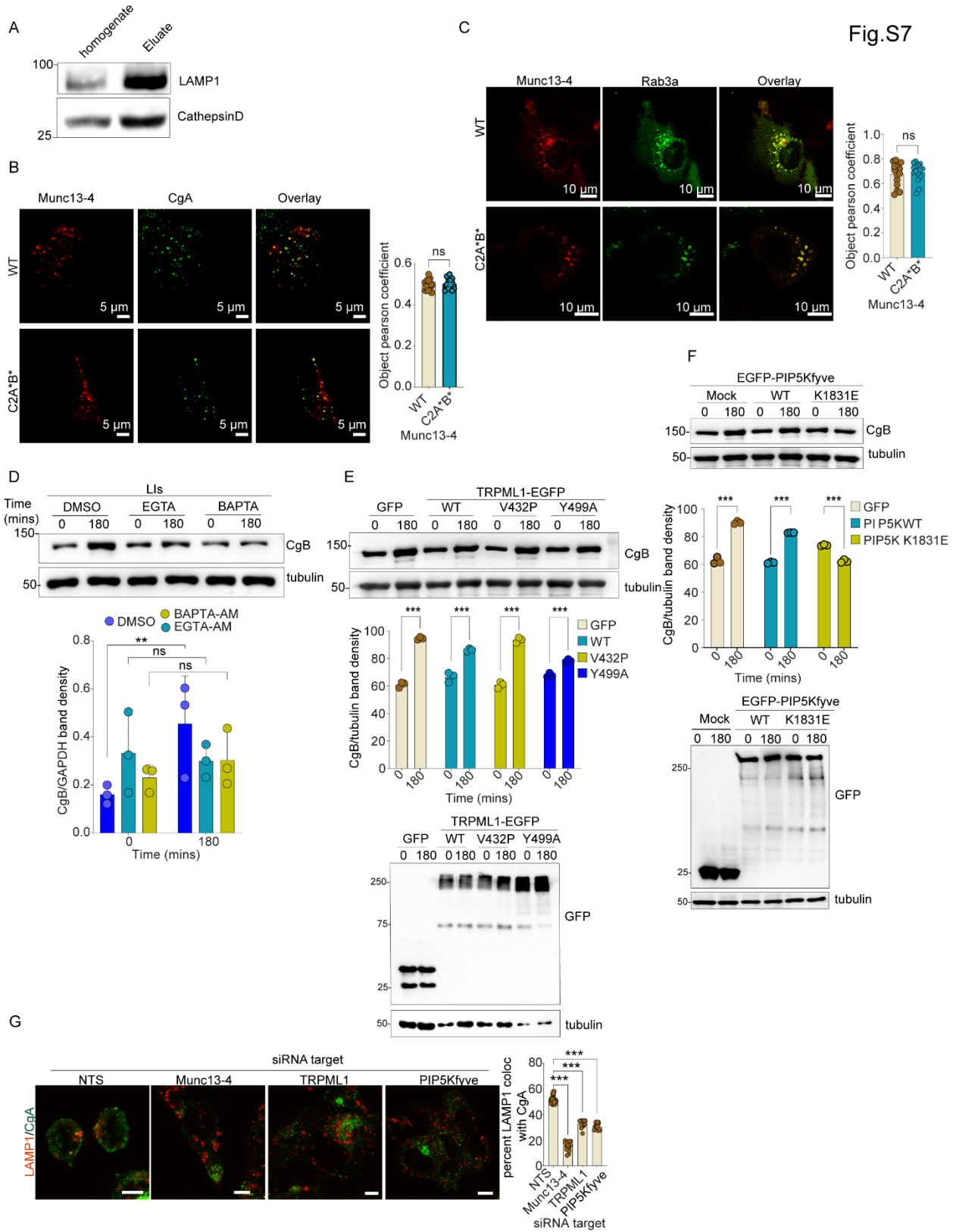
Fig. S6

A



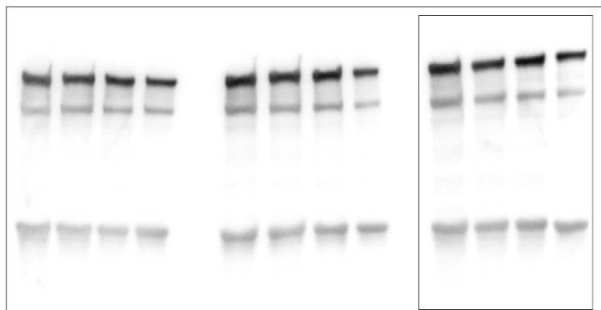
**Fig S6. Munc13 -4 does not interact with ESCRT-I.** A. Lysates of BON cells co-expressing GFP-tagged ESCRT proteins TSG101, VPS37B, VPS37C, and Flag-tagged Munc13-4 were immunoprecipitated with GFP nanobodies. Pull-downs were subjected to western blot analysis using HA or Flag antibodies.

Fig.S7



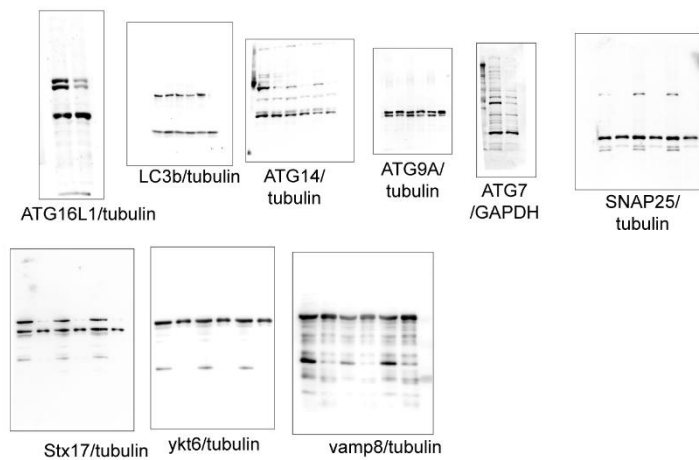
**Fig S7. Munc13-4 mediated heterotypic fusion fueled by calcium.** A Western blot analysis of ~2 percent of homogenate and ~4 percent equivalent enriched lysosomal fraction. B-C. BON cell co-expressed with WT mcherry-Munc13-4 or C2A\*B\* mcherry-Munc13-4 and CgA-EGFP/EGFP-Rab3a. Cells were imaged using a TIRF microscope. Colocalization of Munc13-4 with CgA or Rab3a (n= > 15, mean  $\pm$  SD, ns). D. BON cells were treated with DMSO, EGTA-AM, & BAPTA-AM for 30 min followed by incubation with LIs for the indicated time. Western blot analysis of CgB in cell lysates from three independent experiments was conducted (mean  $\pm$  SD. \*\* p <0.001, ns). E. Activation of TRPML1 channel by PI(3,5)P<sub>2</sub>. BON cells expressing GFP-tagged WT TRPML1 or TRPML variants V432P or Y499A and cells treated with LIs for the indicated time. Western blot analysis of CgB in cell lysates from three independent experiments was conducted (mean  $\pm$  SD, \*\*\*p <0.001). F. BON cells expressing WT PIP5Kfyve or kinase-dead variant PIP5Kfyve-K1831E and cells were treated LI for the indicated time. Western blot analysis of CgB in cell lysates from three independent experiments was conducted (mean  $\pm$  SD, \*\*\*p <0.001). G. BON stable cells expressing CgA-EGFP were treated with indicated siRNAs for 72 hours. The cells were then fixed and immunostained for LAMP1 antibody. Quantitation of colocalization of endogenous LAMP1 (red) with CgA (green) (N=3, n= > 15, mean  $\pm$  SD, \*\*\*p <0.001). A significant reduction in LAMP1 and CgA was observed in Munc13-4, TRPML1, and PIP5Kfyve depleted samples compared to NTS (Scale Bar, 5  $\mu$ m).

Fig S1 A



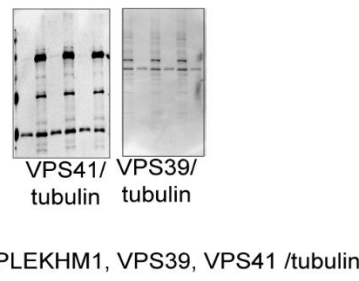
**Figure S1A – Full-blot images.** In some instances, blot images were digitally rotated to straighten bands for cropping. The approximate area cropped for the main figure is shown with a box. All samples were run on the same gel, and target antigens and housekeeping controls were probed on the same membrane.

Fig S2C



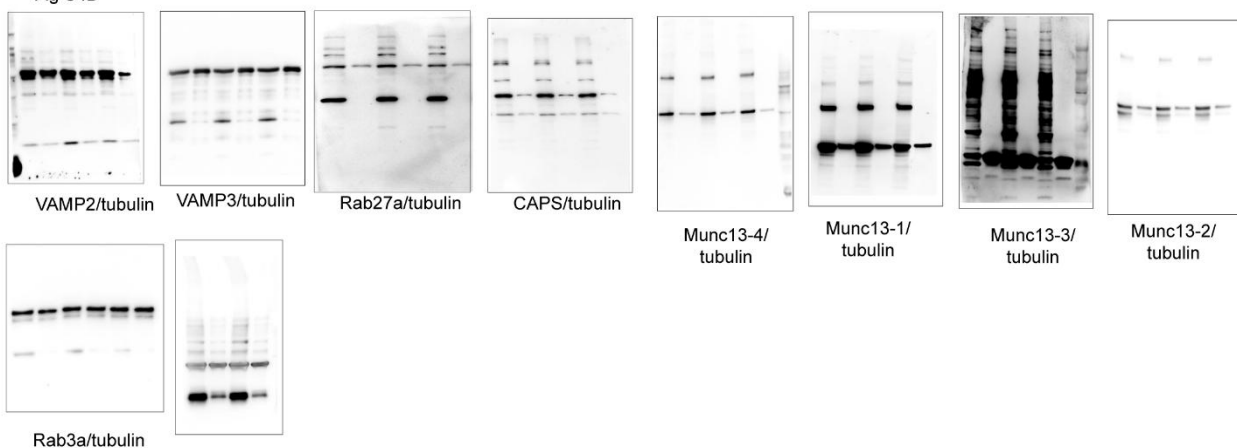
**Figure S2C – Full-blot images.** In some instances, blot images were digitally rotated to straighten bands for cropping. All samples were run on the same gel, and target antigens and housekeeping controls were probed on the same membrane

Fig S3A



**Figure S3A – Full-blot images.** In some instances, blot images were digitally rotated to straighten bands for cropping. All samples were run on the same gel, and target antigens and housekeeping controls were probed on the same membrane.

Fig S4D



**Figure S4D – Full-blot images.** In some instances, blot images were digitally rotated to straighten bands for cropping. All samples were run on the same gel, and target antigens and housekeeping controls were probed on the same membrane. The Munc13-3 blot shown at high contrast corresponds to the image displayed in the supplement.

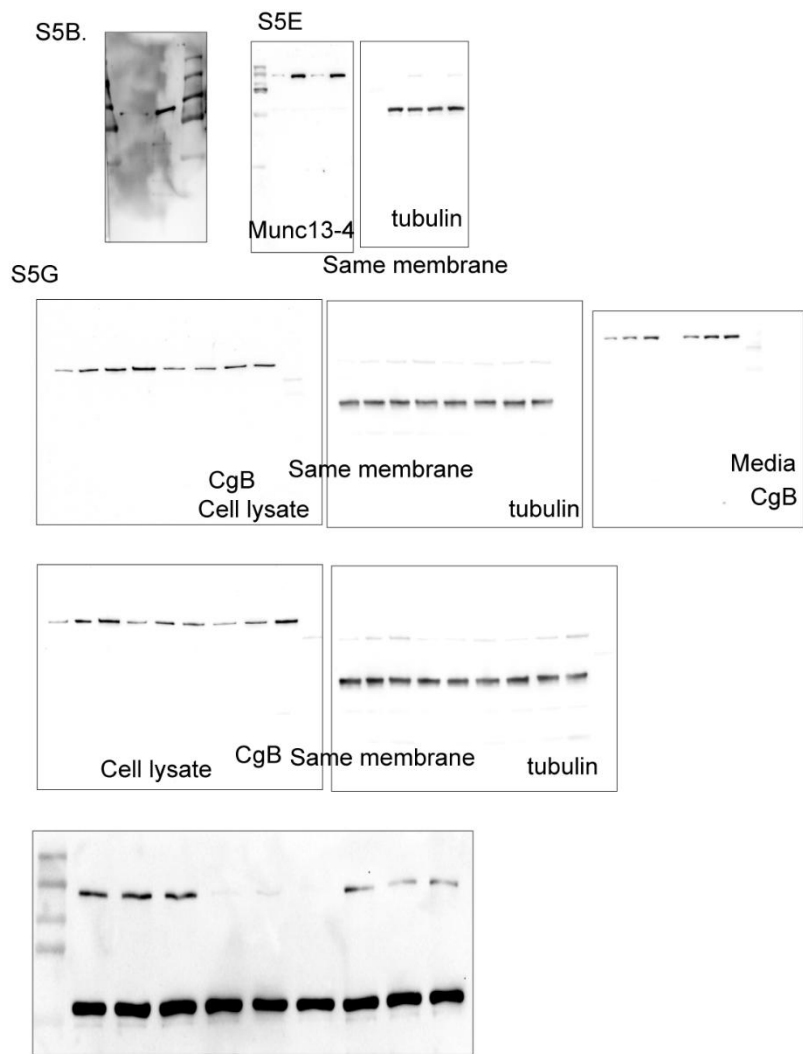
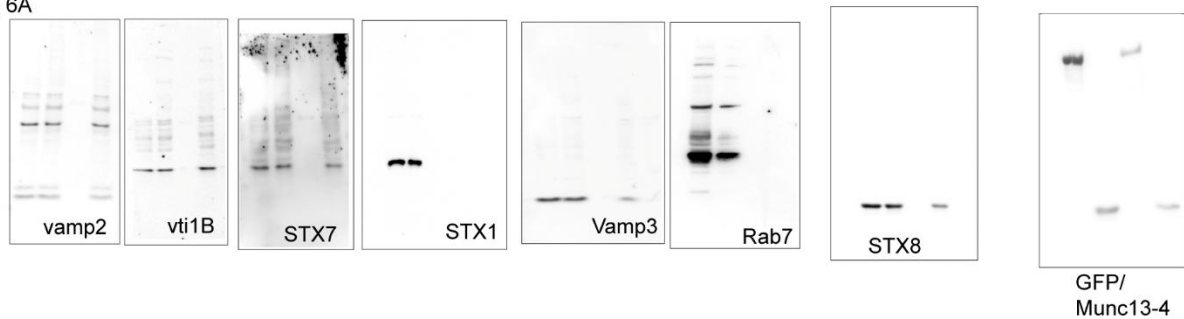
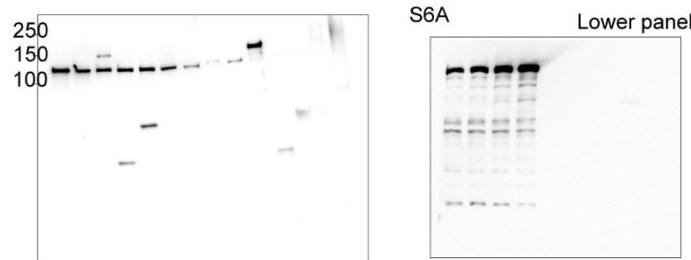


**Figure S5B,E,G – Full-blot images.** In some instances, blot images were digitally rotated to straighten bands for cropping. All samples were run on the same gel, and target antigens and housekeeping controls were probed on the same membrane.

Fig 6A



6B lower blot



S6A Lower panel

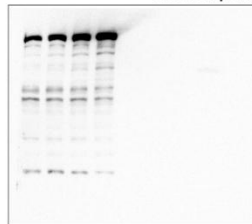


**Figure S6A-B – Full-blot images.** In some instances, blot images were digitally rotated to straighten bands for cropping. All samples were run on the same gel, and target antigens.

Fig S7D



Fig S7F bottom

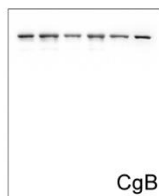


**Figure S7D-F – Full-blot images.** In some instances, blot images were digitally rotated to straighten bands for cropping. All samples were run on the same gel, and target antigens. All samples were run on the same gel, and target antigens and housekeeping controls were probed on the same membrane.